Combined experimental and theoretical studies of the elimination kinetic of 2-methoxytetrahydropyran in the gas phase

ARTICLE *in* JOURNAL OF PHYSICAL ORGANIC CHEMISTRY · DECEMBER 2010

Impact Factor: 1.38 · DOI: 10.1002/poc.1681

6 AUTHORS, INCLUDING:

Mora J.R
Venezuelan Institute for Scientific Research
52 PUBLICATIONS **148** CITATIONS
SEE PROFILE

Edgar alexander Marquez
Universidad de Oriente (Venezuela)
23 PUBLICATIONS **57** CITATIONS
SEE PROFILE

Tania Cecilia Cordova-Sintjago
University of Florida
99 PUBLICATIONS **256** CITATIONS
SEE PROFILE

Gabriel Chuchani
Venezuelan Institute for Scientific Research
245 PUBLICATIONS **1,224** CITATIONS
SEE PROFILE

Research Article

Journal of Physical Organic Chemistry

Received: 20 October 2009, Revised: 16 December 2009, Accepted: 16 December 2009, Published online in Wiley Online Library: 26 February 2010

(wileyonlinelibrary.com) DOI 10.1002/poc.1681

Combined experimental and theoretical studies of the elimination kinetic of 2-methoxytetrahydropyran in the gas phase

Felix Rosas[a], Rosa M. Domínguez[a], José R. Mora[a], Edgar Marquez[a], Tania Córdova[b] and Gabriel Chuchani[a]*

The products formed in 2-methoxytetrahydropyran elimination reaction in the gas phase are 3, 4-dihydro-2H-pyran and methanol. The kinetic study was carried out in a static system, with the vessels deactivated with allyl bromide, and the presence of the free radical suppressor toluene. Temperature and pressure ranges were 400–450 °C and 25–83 Torr, respectively. The process is homogeneous, unimolecular, and follows a first-order rate law. The observed rate coefficient is represented by the following equation: log k (s^{-1}) = (13.95 ± 0.15) − (223.1 ± 2.1) (kJ mol^{-1}) (2.303RT)$^{-1}$. The reactant exists mainly in two low energy chair-like conformations, with the 2-methoxy group in axial or equatorial position. However, the transition state (TS) for the elimination of the two conformers is the same. Theoretical calculations of this reaction were carried for two possible mechanisms from these conformations by using DFT functionals B3LYP, MPW1PW91, and PBE with the basis set 6-31G(d,p) and 6-31G++(d,p). The calculation results demonstrate that 2-methoxytetrahydropyran exists mainly in two conformations, with the 2-methoy group in axial or equatorial position, that are thermal in equilibrium. The average thermodynamic and kinetic parameters, taking into account the populations of the conformers in the equilibrium, are in good agreement with experimental values at B3LYP/6-31++(d,p) level of theory. Copyright © 2010 John Wiley & Sons, Ltd.

Supporting information may be found in the online version of this paper.

Keywords: DFT calculations; gas-phase elimination; kinetics; 2-methoxytetrahydropyran

INTRODUCTION

The gas phase thermal decomposition of several ketals (Scheme 1) was first reported by Molera *et al.*[1–5] In this respect, ethylal decomposed via radical mechanism, while dimethyl and diethyl acetals were believed to undergo rearrangement reactions.[1] In the case of dimethyl acetal, up to 50% reaction, a parallel elimination was found to occur as depicted in reaction (1).

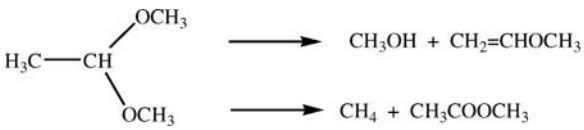

(1)

Again, Molera and his collaborators[2,3] examined the gas-phase pyrolysis of methylal (472–520 °C.)[2] and propylene methylal (512–572 °C.).[3] Because of product formation, these reactions were considered to proceed through a biradical mechanism. Later, methylal decomposition was reexamined in a flow system at 600–732 °C[4,5] showing a complex radical process.

Participation of the hydrogen atom present at the C_α—H bond or at the C_β—H bond in the transition state (TS) mechanism of gas-phase elimination kinetics of ketals (Scheme 2) was recently suggested to be important.[6] According to this work, an electron-withdrawing group Z at the β-carbon should increase the acidity C_β—H bond for a facile abstraction of the H atom by the alkoxy group.

This work[6] on the elimination kinetics of 2, 2-diethoxy ethylamine and 2, 2-diethoxy-*N*,*N*-diethyl ethylamine in the gas phase, at 320–380 °C and 40–150 Torr, proved that these reactions are homogeneous, unimolecular, and follow

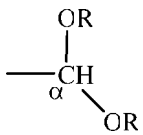

Scheme 1.

* *Correspondence to: G. Chuchani, Centro de Química, Instituto Venezolano de Investigaciones Científicas (I.V.I.C.), Apartado 21827, Caracas, Venezuela. E-mail: chuchani@ivic.ve*

a *F. Rosas, R. M. Domínguez, J. R. Mora, E. Marquez, G. Chuchani*
Centro de Química, Instituto Venezolano de Investigaciones Científicas (I.V.I.C.), Apartado 21827, Caracas, Venezuela

b *T. Córdova*
Escuela de Química, Facultad de Ciencias, Universidad Central de Venezuela, Apartado 1020-A, Caracas, Venezuela

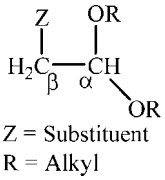

Scheme 2.

a first-order rate law. These reactions involved two parallel reactions. 2, 2-Diethoxy ethylamine yielded (*Step* 1) ethanol and the corresponding unstable intermediate 2-ethoxyethenamine. This intermediate decomposed (*Steps* 3, 4*)* to ethylene, CO, and the corresponding amine. *Step* 2 was found to give, in a lesser amounts, ethane and the corresponding ethyl ester of an α-amino acid [reaction (2)]. These results suggest the H of the C_β—H to participate better than the C_α—H bond in assisting the elimination of ethanol.

RESULTS AND DISCUSSION

The products' formation in the gas-phase elimination of 2-methoxytetrahydropyran, in a static system seasoned with allyl bromide and inhibited with toluene, is described in reaction (3).

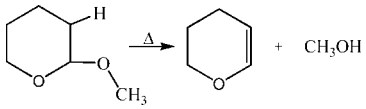

(3)

The experimental stoichiometry for reaction (3) was examined by comparing the amount of decomposition of the substrate 2-methoxytetrahydropyran calculated from pressure measurements with that obtained from gas-chromatographic (GC) analyses of methanol (Table 1). Figure 1 depicts the kinetic profile of the elimination process of this substrate.

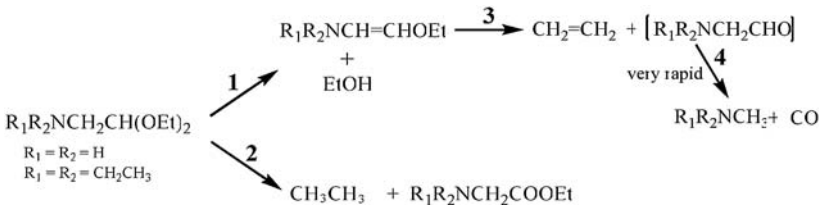

(2)

In spite of the little information on the gas-phase elimination kinetics of ketals, it seemed interesting to study a ketal with one of the oxygen atoms belonging to a cyclic system as a heterocyclic molecule. In this respect, the substrate to examine is 2-methoxytetrahydropyran. The results that may be obtained in this work may lead to additional investigations on the gas-phase elimination kinetics of cyclic ketal type of structure in compounds such as dioxalanes and 1,3-dioxanes. To formulate a reasonable mechanism for the gas-phase elimination kinetic of 2-methoxytetrahydropyran, a theoretical study at DFT computational levels has been undertaken, and to compare the kinetics and thermodynamic parameters of activation with those of the experimental values.

Additional confirmation of the stoichiometry of reaction (3) was made by carrying out the decomposition process until no further pressure increase was obtained. The average ratio of the final pressure, P_f, to the initial pressure, P_0, was found at six different temperatures and ten half-lives to be 2 (Table 2). The theoretical stoichiometry demands $P_f = 2P_0$.

The homogeneity of this elimination reaction was examined under the chain suppressor toluene in a vessel with a surface-to volume ratio of 6.2 cm^{-1} times greater than that of a normal vessel which equal to 1. The packed and unpacked clean Pyrex vessels had a significant effect on the rates. However, when the packed and unpacked vessels are seasoned with allyl bromide, no significant effect on the rate coefficient of

Table 1. Stoichiometry of the reaction[a]

Substrate	Temp (°C)	Time (s)	Reaction (pressure) (%)	MeOH (GC) (%)
2-methoxytetrahydropyran	421.0	60	10.0	9.3
		120	16.7	16.1
		180	23.7	23.4
		300	35.2	34.7
		400	44.4	44.0
		500	53.7	52.1
		600	60.0	59.7
		700	66.7	64.5
		800	73.3	73.0
		900	77.8	77.5

[a] Seasoned vessel and in the presence of toluene inhibitor.

Journal of Physical Organic Chemistry

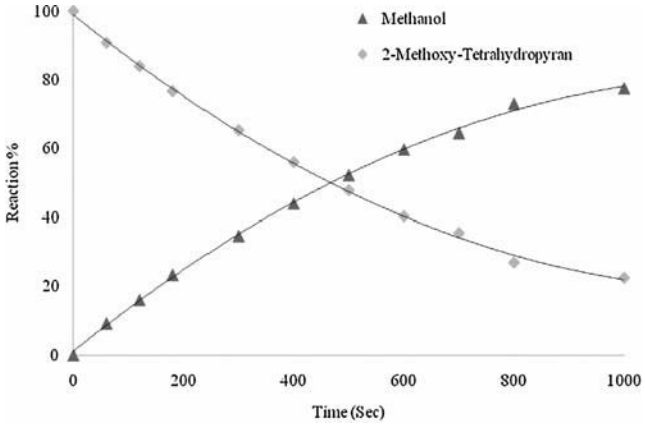

Figure 1. Kinetic profile for gas-phase elimination of 2-methoxytetrahydropyran at 421.0 °C

this ketal was obtained (Table 3). Bearley *et al.*[7] demonstrated that the wall of the reaction chamber had some influence on the determination of the rate coefficient of the thermal decomposition of *t*-butyl chloride, but the result was reproducible when the wall of the chamber was covered with a polymer layer $(C_3H_4)_x$, which is generated by thermal decomposition of allyl bromide.[8]

The effect of the free radical chain inhibitor toluene is shown in Table 4. The absence of toluene suppressor gives a low rate coefficient and this may be due to the fact that one of the products, 3, 4-dihydro-2H-pyran, tends to polymerize. Consequently, the thermal decomposition of 2-methoxytetrahydropyran had to be carried out in the presence of at least an equal amount of the inhibitor. Under this condition no induction period was observed.

The rate coefficients determined in seasoned vessels and in the presence of the inhibitor are independent of the initial pressure of the substrate and calculated from $k_1 = (2.303/t)\log[P_0/(2P_0 - P_t)]$. The first-order plots of log $(2P_0 - P_t)$ against time *t* are satisfactorily linear up to 77% decomposition (Table 5). The rate coefficients are reproducible with a standard deviation not greater than ±5% at a given temperature.

The variation of the first-order rate coefficient with temperature (Table 6, Fig. 2), by using the least-squares procedure and 90% confidence coefficient, leads to the following Arrhenius equation: $\log\ k\ (s^{-1}) = (13.95 \pm 0.15) - (223.1 \pm 2.1)\ (kJ\ mol^{-1})\ (2.303RT)^{-1}$, $r = 0.9996$.

The parameters were calculated using the relation: $(H^{\neq} = E_a - nRT$, Arrhenius equation $k = Ae^{-E_a/RT}$ and Eyring equation: $k = k_B T/he^{-\Delta G^{\neq}/RT}$, $(S^{\neq} = [\ln A - \ln(e^n k_B T/h)]R$. The analysis of the data given in Table 7 suggests a semi-polar concerted four-membered cyclic TS type of mechanism as described in reaction (4). This consideration is derived from the fact that log $A > 13.4$ according to Benson's postulation of the TS Theory.[9,10] Moreover, the small positive entropy of activation suggests the polarization of the C—OCH_3 bond, in the sense $C^{\delta+}\ldots{}^{\delta-}OCH_3$ is rate determining [reaction (4)]. However, to find support or to propose a more reliable argument for a reasonable mechanism of this elimination process, a theoretical calculation study was carried out in order to provide some rational information regarding the molecular decomposition of this reaction.

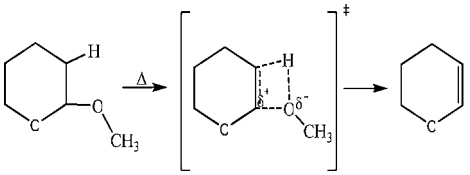

(4)

Table 2. Ratio of final (P_f) to initial (P_0) pressure of the substrate[a]

Substrate	Temp (°C)	P_0 (Torr)	P_f (Torr)	P_f/P_0	Average
2-methoxytetrahydropyran	400.8	30.0	61.0	2.03	2.01 ± 0.02
	410.7	50.0	101.0	2.02	
	421.0	25.5	50.5	1.98	
	431.6	72.0	145.0	2.01	
	441.0	64.0	128.0	2.00	
	451.5	44.0	88.5	2.01	

[a] Seasoned vessel and in the presence of toluene inhibitor.

Table 3. Homogeneity of the elimination reactions[a]

Substrate	Temp (°C)	S/V (cm^{-1})	10^4k (s^{-1})[b]	10^4k (s^{-1})[c]
2-methoxytetrahydropyran	421.0	1	25.89 ± 1.56	14.58 ± 0.38
		6.2	44.01 ± 2.54	14.54 ± 0.37

[a] Presence of toluene inhibitor.
[b] Clean Pyrex vessel.
[c] Deactivated Pyrex vessel with allyl bromide.

Table 4. Effect of toluene inhibitor on rates[a]

Substrate	Temp (°C)	P_0 (Torr)[b]	P_i (Torr)[c]	P_f/P_0	10^4k (s^{-1})
2-methoxytetrahydropyran	421.0	59	0	0	6.16 ± 0.63
		83	100	1.2	14.56 ± 0.34
		54	119	2.2	14.59 ± 0.34
		30	96	3.2	14.51 ± 0.48
		33	132	4.0	14.58 ± 0.53
		27	140	5.2	14.58 ± 0.56

[a] Seasoned vessel.
[b] P_0 = pressure of the substrate.
[c] P_i = pressure of the inhibitor toluene.

Table 5. Invariability of the rate coefficients with initial pressure[a]

Substrate	Temp (°C)	P_0 (Torr)	10^4k (s^{-1})
2-methoxytetrahydropyran	421.0	25	14.51 ± 0.47
		27	14.58 ± 0.56
		30	14.49 ± 0.62
		35	14.59 ± 0.46
		54	14.59 ± 0.38
		62	14.73 ± 0.31
		83	14.56 ± 0.34

[a] Seasoned vessel and in the presence of toluene inhibitor.

COMPUTATIONAL METHOD AND MODEL

Optimized structures of the reactant 2-methoxytretrahydropyran, products methanol and dihydropyran, and TS were obtained using density functional theory (DFT) methods with functionals: B3LYP, MPW1PW91, and PBE the basis set 6-31G(d,p), and 6-31G++(d,p), as implemented in Gaussian 03W.[11] The default options for convergence criteria for the Berny analytical gradient optimization algorithm were used. The TS search was performed using the Quadratic Synchronous Transit (QST) protocol. The nature of stationary points was verified by calculating and diagonalizing the Hessian matrix (force constant matrix). TS structures were characterized by means of normal mode analysis, by having a unique imaginary frequency that is associated with the transition vector (TV). To confirm that the TS structures connect the reactant and products in the reaction path, intrinsic reaction coordinate (IRC) calculations were carried out.

Thermodynamic quantities such as zero-point vibrational energy (ZPVE), temperature corrections [$E(T)$], and absolute entropies [$S(T)$] were obtained from frequency calculations. Temperature corrections and absolute entropies were obtained assuming ideal gas behavior from the harmonic frequencies and moments of inertia by standard methods using average temperature and pressure values within the experimental range.[12] Scaling factors for frequencies and zero-point energies for use are taken from the literature.[13–15]

The first-order rate coefficient $k(T)$ was calculated using the TST[16] and assuming that the transmission

Table 6. Variation of rate coefficients with temperature

Substrate	Temperature (°C)	10^4k (s^{-1})
2-methoxytetrahydropyran	400.8	4.68 ± 0.03
	410.7	8.22 ± 0.17
	421.0	14.58 ± 0.01
	431.6	25.42 ± 0.07
	441.0	44.35 ± 0.23
	451.6	75.44 ± 0.04

Journal of Physical Organic Chemistry

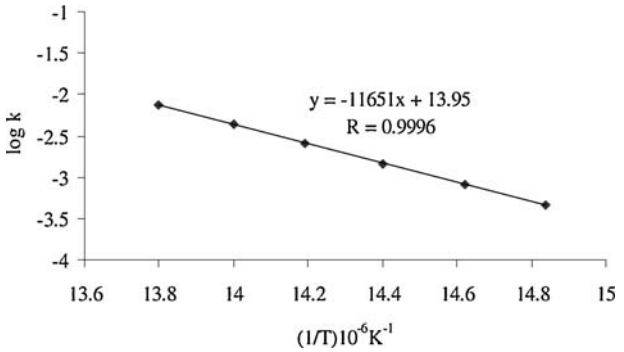

Figure 2. Graphic representation of the Arrhenius plots for the gas-phase elimination of 2-methoxytetrahydropyran

coefficient is equal to 1, as expressed in the following expression:

$$k(T) = (k_B T/h)\, e^{-\Delta G^{\#}/RT}$$

where $\Delta G^{\#}$ is the Gibbs free energy change between the reactant and the TS and k_B, h are the Boltzmann and Planck constants, respectively.

$\Delta G^{\#}$ was calculated using the following relations:

$$\Delta G^{\#} = \Delta H^{\#} - T\Delta S^{\#} \text{ and}$$
$$\Delta H^{\#} = V^{\#} + \Delta ZPVE + \Delta E(T)$$

where $V^{\#}$ is the potential energy barrier, ΔZPVE accounts for the differences of ZPVE between the TS and the reactant, and $\Delta E(T)$ represents the contribution of thermal energy at a given temperature.

THEORETICAL RESULTS

Kinetic and thermodynamic parameters

The thermal elimination reaction from 2-methoxytetrahydropyran was studied to propose a reasonable mechanism. In this elimination, the unimolecular mechanism was considered. We did not carry out calculations considering a radical rupture because it is not consistent with the experimental conditions, which uses free radical inhibitor. Also, the option of ionic mechanism was not studied because this is very unlikely in the gas phase. For the unimolecular mechanism, calculations were carried out in view of the two most important conformers of the reactant, i.e., equatorial–axial. We obtained the TS structure using the QST2 method and verified the structure by means of normal mode analysis and IRC calculations. Frequency calculations allowed obtaining thermodynamic quantities to estimate activation parameters and compare them with the experimental values. The calculated parameters for these eliminations are reported in Table 8. Temperature corrections were carried out at the average experimental conditions ($T = 400\,^{\circ}C$). 2-Methoxytetrahydropyran exists mainly in two chair-like conformations with the 2-methoxy group in the axial or equatorial position (Fig. 3). The free energy difference for these two conformations in equilibrium is 16 kJ mol^{-1} favoring the axial conformer. The difference in electron density causes the equatorial conformers to have a greater dipole moment (2.41 D, PM3 level) than the axial (0.53 D, PM3) explaining the difference in the stability of the two conformers.

The reaction mechanism was studied by taking into consideration the two conformations for the methoxy group as shown in reactions (5) and (6). The calculated thermodynamic parameters for the conformers are shown in (Table 8).

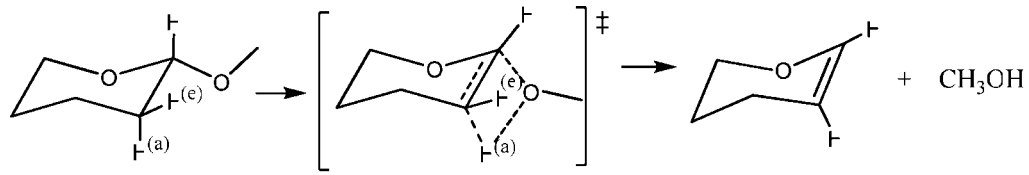

(5)

equatorial

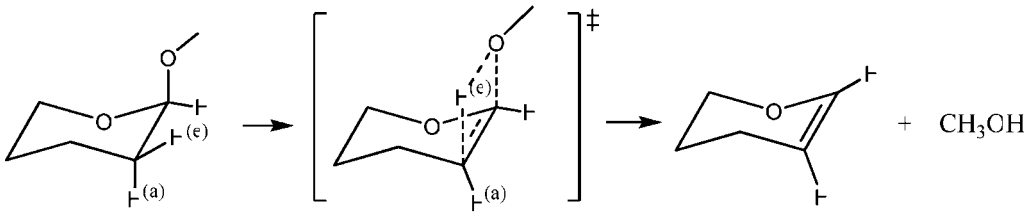

(6)

axial

(e) = equatorial; (a) = axial

Table 7. Kinetic and thermodynamic parameters at 400 °C

Substrate	E_a (kJ mol^{-1})	log A (s^{-1})	ΔH≠!(kJ mol^{-1})	ΔS≠!(J mol^{-1} K^{-1})	ΔG≠ (kJ mol^{-1})
2-methoxytetrahydropyran	223.1 ± 2.1	13.95 ± 0.15	217.5	7.1	212.8

Table 8. Calculated thermodynamic parameters of the equatorial and axial conformers of 2-methoxytetrahydropyran at 400 °C, and the corresponding TS

	H(Hartree/Particle)	*G*(Hartree/Particle)	*S* (Cal mol^{-1} K^{-1})
B3LYP/6–31G(d,p)			
R-axial	−386.102307	−386.243783	131.884
R-equatorial	−386.097457	−386.237886	130.907
TS-axial	−386.004659	−386.154523	139.702
TS-equatorial	−386.004666	−386.154784	137.965
B3LYP/6-31++G(d,p)			
R-axial	−386.113178	−386.253901	131.182
R-equatorial	−386.112292	−386.253053	131.217
TS-axial	−386.021440	−386.170831	139.262
TS-equatorial	−386.024556	−386.175392	132.814
MPW1PW91/6–31G(d,p)			
R-axial	−386.005858	−386.145309	129.996
R-equatorial	−385.997617	−386.138994	131.791
TS-axial	−385.903848	−386.050935	137.114
TS-equatorial	−385.906927	−386.058018	138.252
MPW1PW91/6–31++G(d,p)			
R-axial	−386.014650	−386.154513	130.380
R-equatorial	−386.009522	−386.151916	132.693
TS-axial	−385.920361	−386.070886	140.320
TS-equatorial	−385.920360	−386.071114	137.812
PBE/6-31G(d,p)			
R-axial	−385.615664	−385.75894	133.562
R-equatorial	−385.607762	−385.752681	135.093
TS-axial	−385.528859	−385.679997	140.891
TS-equatorial	−385.528721	−385.681859	141.534
PBE/6-31++G(d,p)			
R-axial	−385.631289	−385.775145	134.092
R-equatorial	−385.624020	−385.770337	136.396
TS-axial	−385.549390	−385.701996	142.259
TS-equatorial	−385.549393	−385.701990	141.327

To estimate the reaction parameters, it is necessary to take into consideration that the reactant exists mainly in two conformers: axial and equatorial in thermal equilibrium.

The free energy of the reactant is the free energy of the whole equilibrium population.[17] According to the equation:

$$G^o[A] = -\mathrm{RT}\ln \sum_{i\varepsilon[A]} \mathrm{e}^{-G^o i/\mathrm{RT}}$$

where [*A*] represents all configurations of the system. Similarly, the free energy of the TS depends on the equilibrium population. To calculate the average parameters, we have considered the two major reactant conformations, i.e, equatorial and axial and the two corresponding TS configurations originated from the two conformers of the reactant. The two TS configurations are degenerate (description of the TS structural parameters is given in the next section).

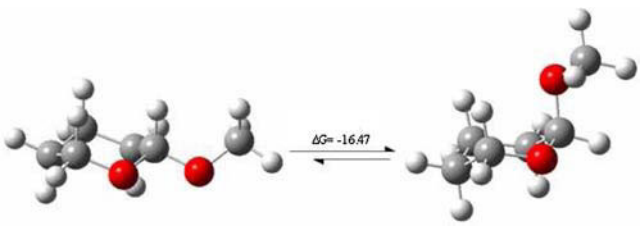

Figure 3. Conformational equilibrium configuration between equatorial and axial structures at 400 °C

The free energy of activation can be calculated as the free energy change between the averages for the TS and reactant. In a similar manner, all activation parameters have been calculated. Average values are reported in Table 9.

The calculated averages presented in Table 9 are in better agreement with experimental values. Better values were obtained using the B3LYP/6-31++G (d,p) method. The inclusion of diffuse functions for B3LYP considerably improves the calculated parameters.

The agreement in the energy of activation together with the experimental entropy of activation suggests a four-membered TS with a loose structure characterized by elongated bonds. Characterization of the TS was carried out in order to verify this hypothesis and to provide a description of the reaction mechanism. The relative energies of the species in this study are plotted in Fig. 4.

Table 9. Calculated *average* kinetic and thermodynamic parameters of activation for 2-methoxytetrahydropyran elimination at 400 °C

	E_a (kJ mol^{-1})	log A (s^{-1})	$\Delta H^{\neq}$ (kJ mol^{-1})	$\Delta G^{\neq}$ (kJ mol^{-1})	$\Delta S^{\neq}$ (J mol^{-1} K^{-1})
Experimental average parameter	223.9 ± 2.1	13.95	218.3	213.55	7.06
B3LYP/6-31G(d,p)	248.7	14.99	243.1	217.9	27.02
B3LYP/6-31++G (d,p)	235.2	13.93	229.6	203.5	6.64
MPW1PW91/6-31G(d,p)	243.7	15.14	238.1	212.6	29.78
MPW1PW91/6-31++G (d,p)	239.2	14.69	233.6	210.8	21.27
PBE/6-31G(d,p)	213.0	14.87	207.4	185.8	24.62
PBE/6-31++G (d,p)	201.3	14.65	195.8	178.9	20.11

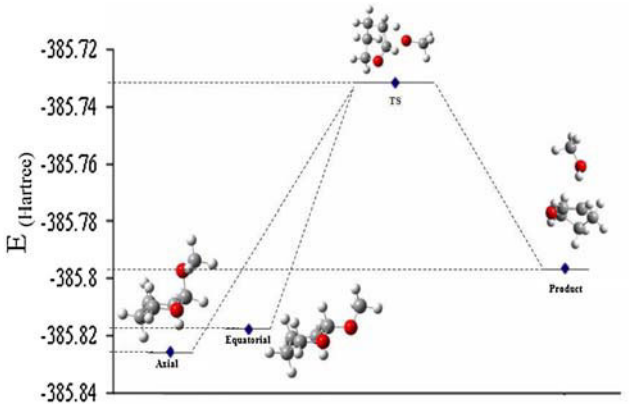

Figure 4. Energies of all the two reactant conformers, TS and products using PBE functional

Transition state and mechanism

The TSs for the two mechanisms leading to products formation were determined. We have selected the B3LYP/6-31G(d,p) structures for the axial path and PBEPBE/6-31G(d,p) structures for the equatorial path for the geometrical parameters. The geometrical parameters of all molecules are similar with all the methods used for each mechanism. The fully optimized structures for reactants, TS and products for the axial mechanism from calculations at B3LYP/6-31++G(d,p) level of theory and the corresponding optimized structures at PBEPBE/6-31G(d,p) for the equatorial mechanism are shown in Fig. 5. Geometrical parameters for the two mechanisms are given in Table 10. Scheme 3 shows the atom numbers of the TS configurations for clarity in the subsequent discussion of the TS structural parameters, charges, and bond order analysis.

The optimized TS structures for the two mechanisms are four-membered ring geometry, close to planar configuration, as seen from the dihedral values. The axial conformer has a higher dipole moment and is more stable than the equatorial (Fig. 4).

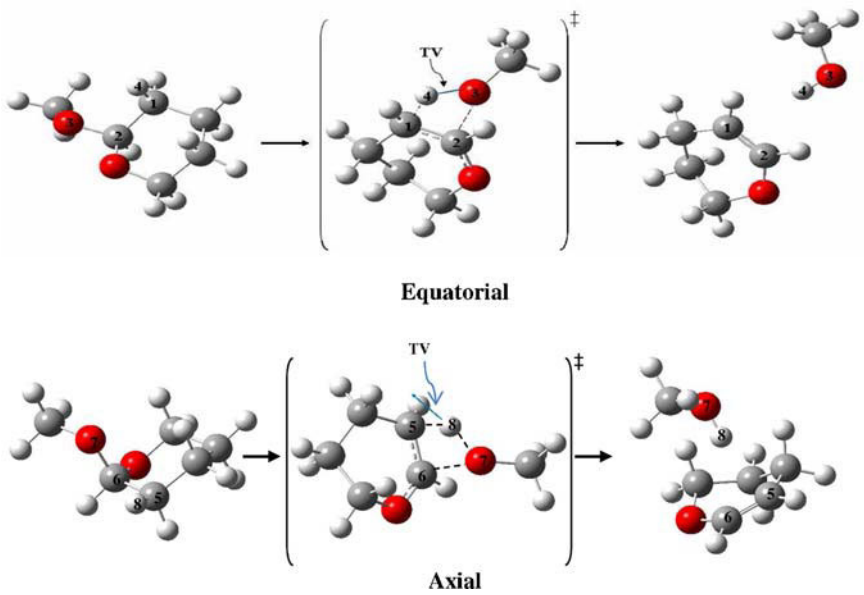

Figure 5. Structures of the optimized reactant (left), transition state TS (center), and products (right) optimized for the two proposed reaction mechanisms

Table 10. Structural parameters for optimized reactant (R), transition state (TS), and products (P) from 2-methoxytetrahydropyran elimination. Atom distances are in Å and dihedral angles in degrees

		Equatorial		
		Atom distances (Å)		
	C_1—C_2	C_2—O_3	O_3—H_4	H_4—C_1
R	1.533	1.420	2.561	1.103
TS	1.442	2.118	1.361	1.303
P	1.355	3.362	0.983	2.247
		Dihedrals		
	C_1—C_2—O_3—H_4	C_2—O_3—H_4—C_1	O_3—H_4—C_1—C_2	H_4—C_1—C_2—O_3
TS	−4.081	6.267	−7.890	3.649
		Imaginary frequency (cm^{-1})		
TS	1483.11			
		Axial		
		Atom distances (Å)		
	C_5—C_6	C_6—O_7	O_7—H_8	H_8—C_5
R	1.532	1.420	2.561	1.103
TS	1.442	2.118	1.361	1.303
P	1.355	3.362	0.983	2.247
		Dihedrals		
	C_5—C_6—O_7—H_8	C_6—O_7—H_8—C_5	O_7—H_8—C_5—C_6	H_8—C_5—C_6—O_7
TS	−4.080	6.267	−7.890	3.649
		Imaginary Frequency (cm^{-1})		
TS	1164.45			

Because of the small barrier between the two conformers, they exist in equilibrium; consequently the axial conformer will change to equatorial to react. The imaginary frequency is associated with the hydrogen transfer from the C_β to the oxygen atom of the methoxy moiety. In both TS the C_1—C_2 is shortened from 1.55 to 1.44 Å in the TS as the double bond is formed, accompanied by an elongation of C_2—O_3 bond from 1.42 to 2.12 Å, which breaks to form methanol, decrease in the O_3—H_4 distance from 2.56 to 1.36 Å as the hydrogen is being transferred and increase in the H_4—C_1 distance from 1.10 to 1.30 Å indicating bond breaking.

IRC calculations were carried out to verify the nature of the TS in the reaction coordinate connecting reactant and products. IRC plots are given as supplementary data (Figs S6 and S7). The above result suggests that the two mechanisms are similar regarding structural parameters. Both paths occur through four-membered cyclic TS structure with considerable C_2—O_3 bond breaking and hydrogen transference from C_β to the methoxy oxygen atom.

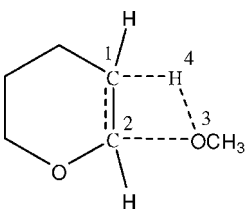

Scheme 3.

NBO charges

The changes in electron density distribution leading to the formation of methanol and dihydropyrame from 2-methoxytetrahydropyrane were followed using NBO charges and bond order analysis. NBO charges are shown in Table 11. Atoms numbering refer to Scheme 3.

Charges in the reactant are similar in either conformation. However, C_1 is more negative when the methoxy group is in the equatorial position and C_2 is more positive; also, in the axial conformation oxygen is higher in electron density compared to the equatorial. Going from the reactant to the TS that leads to the products, in both mechanisms there is an increase in electron density at C_1 and O_3, C_2 becomes less positive and the hydrogen being transferred is more positive. Differences in electron distribution are very small in the two TS, implying analogous TS.

Bond order analysis

NBO bond order calculations[18–20] have been used to study the reaction progress along the reaction pathway. Wiberg bond indexes[21] were computed using the natural bond orbital NBO program[22] as implemented in Gaussian 03W. These indexes can be used to estimate bond orders from population analysis. Bond breaking and making processes involved in the reaction mechanism are monitored by means of the Synchronicity (Sy) concept proposed by Moyano *et al.*[23] defined by the expression:

$$Sy = 1 - \left[\sum_{i=1}^{n} |\delta Bi - \delta Bav| / \delta Bav\right] / 2n - 2$$

The parameter n is the number of bonds directly involved in the reaction and the relative variation of the bond index is

Table 11. NBO charges of the atoms involved in 2-methoxytetrahydropyran thermal decomposition

2-Methoxytetrahydropyran			
	R	TS	P
		Equatorial	
C_1	−0.547	−0.633	−0.393
C_2	0.381	0.296	0.083
O_3	−0.542	−0.730	−0.744
H_4	0.259	0.400	0.481
		Axial	
	R	TS	P
C_1	−0.533	−0.645	−0.405
C_2	0.352	0.291	0.088
O_3	−0.568	−0.702	−0.753
H_4	0.266	0.407	0.487

obtained from

$$\delta B_i = [B_i^{TS} - B_i^{R}]/[B_i^{P} - B_i^{R}]$$

The superscripts R, TS, P represent reactant, transition state, and product respectively.

The evolution in bond change is calculated as: $\%E_v$ and the average value is calculated from

$$\delta B\text{av} = 1/n \sum_{i=1}^{n} \delta Bi$$

Wiberg bond indexes B_i were calculated for those bonds involved in methanol elimination from 2-methoxytetrahydropyran, i.e., C_1, C_2, O_3, H_4. Other bond changes are minor and were not considered in the analysis.

Wiberg bond indexes in Table 12 show that for both mechanisms, the progress along the different reaction coordinates is similar. For both paths, the most advanced reaction coordinate is the breaking of the C_2—O_3 bond (60–62%). Other events show less progress in the TS, that is, the TS is late with respect to C—O breaking and early in hydrogen transference and C_1—C_2 bond order changes, revealing asynchronous process. The synchronicity parameter has been used to characterize synchronic and non-synchronic reactions. The parameter varies between 0 and 1, where 1 is assigned to a fully synchronic process. Unimolecular reactions occurring in a concerted fashion show different synchronicity parameters implying variations in the TSs electron distribution associated with the molecular structure and the substituents. We have found that the two proposed mechanisms differ slightly, with the axial path being less a-synchronous (Sy = 0.861) than the equatorial (Sy = 0.847).

The elimination reaction proceeds through a four-membered TS, and is essentially identical in both cases either considering the axial or equatorial conformers of the reactant, characterized by an advanced C—O bond breaking. This is also seen in the geometrical parameters and NBO charges.

Table 12. NBO analysis for 2-methoxytetrahydropyran thermal decomposition. Wiberg bond indexes (B_i), % evolution through the reaction coordinate ($\%E_v$) are shown for R, TS, and P. Average bond index variation (δb_{av}) and synchronicity parameter (Sy) are also reported

Methanol formation					
	C_1—C_2	C_2—O_3	O_3—H_4	H_4—C_1	S_y
			Equatorial		
B_i^R	0.9900	0.9267	0.0029	0.8950	0.847
B_i^{ET}	1.2310	0.3508	0.2718	0.5065	
B_i^P	1.7978	0.0063	0.7294	0.0155	
$\%E_v$	29.8	62.6	37.0	44.2	
			Axial		
B_i^R	0.9961	0.9172	0.0012	0.8959	0.861
B_i^{ET}	1.2328	0.3725	0.2906	0.4765	
B_i^P	1.7826	0.0091	0.7138	0.0246	
$\%E_v$	30.1	60.0	40.6	48.1	

CONCLUSIONS

The products of the thermal elimination of 2-methoxytetra-hydropyran are methanol and dihydropyran. The reaction is unimolecular, homogeneous, and follows first-order reaction kinetics. The observed rate coefficient is represented by the equation: $\log\ k\ (s^{-1}) = (13.95 \pm 0.15) - (223.1 \pm 2.1)\ (kJ\ mol^{-1})\ (2.303RT)^{-1}$. The reactant 2-methoxytetra-hydropyran exists in two low energy chair-like conformations, with the 2-methoxy group in axial or equatorial position. Theoretical calculations of this reaction were carried out for two putative mechanisms from the two reactant conformations, using DFT methods. The small energy difference between the conformers, axial–equatorial indicates that they are in thermal equilibrium. Calculated averages of the activation parameters considering the equilibrium populations of reactant and TS are in good agreement with the experimental values. Better parameters were obtained using B3LYP/6-31++G(d,p) method. The use of diffuse function is important in the treatment of this reaction. These results suggest that the two reactant conformers are in equilibrium. NBO charges and bond orders imply that the rate-determining step is the breaking of the C_α—O bond while other reaction coordinates show less progress in the TS, implying the reaction is polar and moderately asynchronous.

EXPERIMENTAL

The substrate 2-methoxytetrydropyran of 98% purity (GC-MS Saturn 2000, Varian, with a DB-5MS capillary column 30 m × 0.53 mm i.d., 0.53 μm film thickness) was acquired from Aldrich. The pyrolysis products, 3,4-dihydro-2H-pyran and methanol, were identified in a GC–MS Saturn 2000, Varian with a DB-5MS capillary column 30 m × 0.25 mm i.d., 0.25 μm. The quantitative analysis of the product methanol (Fisher) was carried out by using a Varian 3700 Gas Chromatograph with a Porapak R (80–100 mesh) column.

Kinetics

The kinetic determinations were performed in a static reaction system as reported[24–26] at each temperature; several runs are carried out in our experiments. According to the static system figure described before,[26] the reaction vessel of approximately 250 ml is enclosed in a thermostatic furnace which is a cylindrical aluminum block 20.5 cm in diameter and 36 cm high with a central circular well 10 cm diameter. A nichrome heating coil of resistance 90 Ω was wound on it after insulation with asbestos. This furnace is united to a glass diaphragm and to a mercury manometer. The substrate for analysis is injected to the reaction vessel with a syringe Perfektum of 1.0 ml through a capillary silicone rubber septum. The increase of pressure in the system due to the thermal decomposition of the substrate causes a small deformation of the glass diaphragm, which is then compensated with the introduction of air by using a valve. The diaphragm lighted by a lamp produces an indicating line which moves from the reference point when pressure increases. The variation of pressure increase seen in the mercury manometer with time is measured with a chronometer. The initial pressure of the reaction at time zero is estimated by extrapolation in a graphic of pressure versus time. The temperatures were determined by using a calibrated iron-constantan thermocouple and measured in a Digital Multimeter Omega 3465B. The temperature was maintained within ±0.2 °C through control with a Shinko DIC-PS 23TR resistance thermometer. The vacuum of this static system is accomplished by a rotatory vacuum pump Hitachi LTD 3VP – C2 and can reach approximately 5.0×10^{-4} Torr. The vacuum may be improved when using the Mercury diffusion pump Edwards EMG 150 W. The pyrolysis products were trapped in the reactant storage reservoir. The amount of substrate used for each reaction was ~0.05–0.1 ml.

Acknowledgements

T.C. thanks the Consejo de Desarrollo Científico y Humanístico (C.D.C.H.) for Grant No. PG-03-00-6499-2006.

REFERENCES

[1] M. Molera, J. Centeno, J. Orza, *J. Chem. Soc.* **1963**, 2234–2241.
[2] M. Molera, J. Fernandez-Biarge, J. Centeno, L. Arévalo, *J. Chem. Soc.* **1963**, 2311–2320.
[3] M. Molera, G. Dominguez, *Anal. Real. Soc. Esp. Fís. y Quim.* **1963**, *11*, 639–648.
[4] M. Molera, G. Pereira, *Anal. Fis. Quim.* **1966**, *62*, 661–666.
[5] M. Molera, G. Pereira, *Anal. Fis. Quim.* **1966**, *62*, 667–675.
[6] J. R. Mora, R. M. Dominguez, A. Herize, M. Tosta, G. Chuchani, *J. Phys. Org. Chem.* **2008**, *21*, 359–364.
[7] D. Brearley, G. Kistiakowsky, C. Stauffer, *J. Am. Chem. Soc.* **1936**, *58*, 43;
[8] A. Maccoll, *J. Chem. Soc.* **1955**, 965.
[9] S. Benson, H. O'Neal, *J. Phys. Chem.* **1967**, *71*, 2903–2921.
[10] S. B. Benson, *Thermochemical Kinetics*, John Wiley & Sons, New York, **1968**.
[11] M. J. Frisch, G. W. Trucks, H. B. Schlegel, G. E. Scuseria, M. A. Robb, J. R. Cheeseman, J. A. Montgomery, Jr., T. Vreven, K. N. Kudin, J. C. Burant, J. M. Millam, S. S. Iyengar, J. Tomasi, V. Barone, B. Mennucci, M. Cossi, G. Scalmani, N. Rega, G. A. Petersson, H. Nakatsuji, M. Hada, M. Ehara, K. Toyota, R. Fukuda, J. Hasegawa, M. Ishida, T. Nakajima, Y. Honda, O. Kitao, H. Nakai, M. Klene, X. Li, J. E. Knox, H. P. Hratchian, J. B. Cross, V. Bakken, C. Adamo, J. Jaramillo, R. Gomperts, R. E. Stratmann, O. Yazyev, A. J. Austin, R. Cammi, C. Pomelli, J. W. Ochterski, P. Y. Ayala, K. Morokuma, G. A. Voth, P. Salvador, J. J. Dannenberg, V. G. Zakrzewski, S. Dapprich, A. D. Daniels, M. C. Strain, O. Farkas, D. K. Malick, A. D. Rabuck, K. Raghavachari, J. B. Foresman, J. V. Ortiz, Q. Cui, A. G. Baboul, S. Clifford, J. Cioslowski, B. B. Stefanov, G. Liu, A. Liashenko, P. Piskorz, I. Komaromi, R. L. Martin, D. J. Fox, T. Keith, M. A. Al-Laham, C. Y. Peng, A. Nanayakkara, M. Challacombe, P. M. W. Gill, B. Johnson, W. Chen, M. W. Wong, C. Gonzalez, J. A. Pople, *Gaussian 03*, Revision C.02, Gaussian, Inc., Wallingford, CT, **2004**.
[12] D. McQuarrie, *Statistical Mechanics*, Harper & Row, New York, **1986**.
[13] J. B. Foresman, A. Frisch, *Exploring Chemistry with Electronic Methods*, 2nd edn, Gaussian, Inc, Pittsburg, PA, **1996**.
[14] Scale factors in http://cccbdb.nist.gov/vibscalejust.asp
[15] Database of Frequency Scaling Factors for Electronic Structure Methods. http://comp.chem.umn.edu/truhlar/freq_scale.htm
[16] S. W. Benson, *The Foundations of Chemical Kinetics*, Mc-Graw-Hill, New York, **1960**.
[17] C. J. Cramer, *Essentials of Computational Chemistry: Theories and Models*, 2nd edn, Chapter 10, John Wiley & Sons, Chichester, **2004**.
[18] G. J. Lendvay, *J. Phys. Chem.* **1989**, *93*, 4422–4429.
[19] A. E. Reed, R. B. Weinstock, F. Weinhold, *J. Chem. Phys.* **1985**, *83*, 735–746.
[20] A. E. Reed, L. A. Curtiss, F. Weinhold, *Chem. Rev.* **1988**, *88*, 899–926.
[21] K. B. Wiberg, *Tetrahedron* **1968**, *24*, 1083–1095.
[22] A. E. Reed, J. E. Carpenter, F. Weinhold, NBO version 3.1.
[23] A. Moyano, M. A. Periclas, E. Valenti, *J. Org. Chem.* **1989**, *54*, 573–582.
[24] A. Maccoll, *J. Chem. Soc.* **1955**, 965–973.
[25] E. S. Swinbourne, *Aust. J. Chem.* **1958**, *11*, 314–330.
[26] R. M. Dominguez, A. Herize, A. Rotinov, A. Alvarez-Aular, G. Visbal, G. Chuchani, *J. Phys. Org. Chem.* **2004**, *17*, 399–408.

